
This manuscript is a non-peer reviewed preprint submitted to EarthArXiv for public posting. It will be shortly submitted to a scientific journal for peer-review and potential publication. As a function of the peer-review process that this manuscript will undergo, its structure and content may change.

Mapping ethylene plumes using satellite high-resolution imaging spectrometers that exploit the SWIR spectrum

Javier Roger^{1,2*}, Adriana Valverde¹, Javier Gorroño¹, Michael Hilker², Zhipeng Pei³, Itziar Irakulis-Loitxate^{1,4}, Luis Guanter^{1,5}

¹Research Institute of Water and Environmental Engineering (IIAMA), Universitat Politècnica de València (UPV), Valencia, Spain.

²Institute of Environmental Physics (IUP), University of Bremen, Bremen, Germany.

³School of Remote Sensing and Information Engineering, Wuhan University, Wuhan, China.

⁴International Methane Emissions Observatory, United Nations Environment Programme.

⁵Environmental Defense Fund, Amsterdam, the Netherlands.

*Now at Institute of Environmental Physics (IUP), University of Bremen, Bremen, Germany.

*To whom correspondence should be addressed; E-mail: jroger@iup.physik.uni-bremen.de

Ethylene (C₂H₄) is an important volatile organic compound that has a negative impact on human health, but space-based monitoring of plumes from this gas remains largely unexplored. Here, we demonstrate, for the first time, that ethylene point-source emissions can be detected and quantified using shortwave infrared (SWIR) imaging spectroscopy, overcoming the spatial limitations of existing thermal infrared observations. As a proof of concept, we apply a matched filter approach to EMIT data and retrieve two ethylene plumes from industrial facilities in Saudi Arabia and Iraq. The emission rate of the first source is consistent with IASI measurements, whereas the second reveals a previously unreported hotspot, highlighting the potential of SWIR imaging spectrometers for high-resolution monitoring of ethylene sources.

Introduction

Ethylene (C₂H₄) is a volatile organic compound that contributes to air pollution as a precursor of tropospheric ozone and formaldehyde, which ultimately has an impact on human health^[1]. It is emitted into the atmosphere from biomass burning, urban activity, and industrial processes, and its production is expected to increase^[2].

Franco et al.^[3] used satellite-based thermal infrared (TIR) measurements from the IASI instrument^[4] and identified over 300 ethylene anthropogenic hotspots. Most of these emissions originated from industry, primarily from the metallurgy, coal, and chemical sectors. Bottom-up emission inventories largely underestimate industrial emissions, and in some cases do not include them. These findings highlight the limitations of current inven-

34 tories and underscore the importance of space-based emission monitoring for supporting
35 effective environmental policies. Even though IASI could identify and quantify all these
36 hotspots, its coarse spatial resolution (> 12 km) is not sufficient to attribute emissions to
37 their corresponding point sources in large industrial hubs. Instruments with finer spatial
38 resolution are required for this task.

39 While ethylene absorption lines in the TIR spectrum are available in public databases,
40 measurements of its absorption in the shortwave infrared (SWIR) are only reported in the
41 literature⁵. From Sharpe et al.⁶, we obtained the ethylene cross section spectrum in the
42 1550–2500 nm spectral range. Figure 1 compares the absorption cross sections of ethy-
43 lene and methane (CH₄), showing features of comparable magnitude. Several satellite
44 imaging spectrometers currently cover this spectral region while providing relatively high
45 spatial resolution. Among these is EMIT⁷, which has a pixel size of 60 m. Since methane
46 plumes can be detected with this instrument^{8,9}, the detection of ethylene plumes may also
47 be feasible, potentially improving the attribution of emissions to individual point sources.

48 [Figure 1 about here.]

49 In this study, we combine the cross section spectrum from Sharpe et al.⁶ with EMIT
50 observations to assess the feasibility of detecting and quantifying ethylene point source
51 emissions from space. To demonstrate this capability, we characterize two plumes origi-
52 nating from industrial areas in Iraq and Saudi Arabia.

53 **Methods and materials**

54 We acquired L1 data from the EMIT instrument, which are publicly available through the
55 mission data portal. The matched filter method¹⁰ was then applied to derive ethylene
56 concentration-path-length enhancement (α) maps, expressed in ppm·m. These maps
57 were subsequently used to identify and quantify point-source emissions.

58 Following Roger et al.,¹¹ multiple iterations and supervised radiance thresholding
59 were added to the basic matched filter implementation. The unit gas absorption spec-
60 trum (K) required by this methodology was derived from high-resolution radiance spectra
61 (0.1 nm). Optical depth spectra were first computed using the HITRAN 2024 line-by-line
62 database¹² and the ARTS radiative transfer model¹³, and subsequently converted into
63 radiance spectra using libRadtran¹⁴. A sea-level surface elevation and a midlatitude sum-
64 mer atmospheric profile from the RFM model¹⁵ were assumed. To account for ethylene
65 absorption, the cross section spectrum from Sharpe et al.⁶ was incorporated into the
66 atmospheric optical depth generated by ARTS. Several radiance spectra were then sim-
67 ulated for different values of α . For simplicity, an infinite ethylene lifetime was assumed,

68 and the same α values used for ammonia (NH₃) in Roger et al.,^[11] were adopted. The
69 K spectrum was generated following Foote et al.,^[16] already accounting for the convolu-
70 tion to the instrument spectral response function and the specific acquisition geometry.
71 We used the 2000–2450 nm spectral range to characterize ethylene, as it contains the
72 strongest absorption features of this gas. In addition, K spectra for CH₄, NH₃, CO₂, and
73 H₂O were generated using the same setup as in Roger et al.^[11], to enable assessment of
74 potential ethylene false positives through comparison with retrievals of other gases.

75 Atmospheric ethylene concentrations were set to zero, as ambient concentrations
76 are typically negligible^[17]. Furthermore, ethylene emissions were assumed to be in the
77 first 500 m above the surface within our reference atmosphere, where a pressure of $P = 1$
78 atm and a temperature of $T = 294$ K were assumed. However, the cross section spectrum
79 from Sharpe et al.^[6] was measured under conditions of $P = 1$ atm and $T = 298.1$ K. To
80 assess the impact of this temperature difference, we performed a test using methane as
81 a reference gas. Methane cross section spectra were generated with the HAPI tool^[18]
82 using $P = 1$ atm and temperatures of $T = 294$ K and $T = 298.1$ K. Following the procedure
83 described above, the corresponding K spectra for the methane case were generated and
84 compared, revealing no significant differences due to this difference in temperature. A
85 similar behavior is therefore expected for ethylene, indicating that the resulting K spectrum
86 is sufficiently accurate for the consistent detection and quantification of ethylene plumes.

87 Ethylene plumes are quantified using the IME method^{[19][20]}, which provides the emis-
88 sion rate (Q) in t h^{-1} . This methodology requires the effective wind speed (U_{eff}), an
89 empirical parameter that relates Q to the mass and spatial extent of the plume. U_{eff}
90 was obtained using a calibration approach similar to that of Guanter et al.,^[21] based on
91 the WRF-LES simulations presented by Gorroño et al.^[22] and located in Zenodo^[23]. This
92 calibration was adapted to the molar mass of ethylene and to the EMIT instrument by con-
93 sidering the typical noise levels of ethylene retrievals. The lower and upper bounds of the
94 noise range were derived from the same regions used by Roger et al.,^[11] for NH₃, and the
95 same emission-rate range was adopted. The resulting calibration is $U_{eff} = 0.48 \cdot U_{10} +$
96 0.59 , where U_{10} is the wind speed at 10 m above the surface, obtained from the GEOS-FP
97 product^[24]. Note that emission rate uncertainty is calculated as in Roger et al.,^[25].

98 Results and discussion

99 In Figure 2, we show ethylene plumes originating from two different sources. One of these
100 emissions (left panel) is located in Yanbu, Saudi Arabia, and is associated with a single
101 source. This source is part of an ethylene hotspot identified by Franco et al.,^[3] as a large
102 petrochemical hub. The higher spatial resolution of EMIT allows us to better constrain
103 the potential emission sources to a much smaller area within the petrochemical complex.
104 An analysis of high-resolution RGB imagery from Google Earth suggests that the plume

105 originates from a flare stack. We estimated an emission rate of $Q = 3.2 \pm 0.9 \text{ t h}^{-1}$, which
106 agrees with the one deduced from IASI with $Q = 0.72 (0.36\text{--}4.28) \text{ t h}^{-1}$. A second plume
107 was detected over another petrochemical complex in Iraq (right panel). This plume also
108 appears to originate from a flare stack, and an emission rate of $Q = 3.7 \pm 1.3 \text{ t h}^{-1}$ was
109 estimated. This region was not previously identified as an ethylene hotspot by Franco
110 et al.,³. Possible explanations include differences in acquisition dates between the IASI
111 observations and our measurements. The study of Franco et al.,³ covered the period from
112 2008 to 2020, whereas the plume detected over Iraq was observed in 2023. Changes in
113 industrial activity may therefore have occurred during this period.

114 [Figure 2 about here.]

115 Additional visual inspection of the CH_4 , CO_2 , NH_3 , and H_2O retrievals was carried
116 out to assess whether the ethylene plumes shown in Figure 2 could be false positives.
117 Part of this assessment is illustrated in Figure 3, where the ethylene retrieval is compared
118 to that of methane. Note that the analyzed sources are marked with red dots. We observe
119 no correlation with other gases, which increases confidence in the ethylene plumes.

120 [Figure 3 about here.]

121 Imaging spectrometers with characteristics similar to those used in this study, in-
122 cluding the AVIRIS family²⁶, EnMAP²⁷, PRISMA²⁸, GF-5 AHSI²⁹, and Tanager-1³⁰, are
123 promising candidates for ethylene plume detection. Upcoming missions such as CHIME³¹,
124 as well as future Carbon Mapper instruments, are also expected to provide valuable ca-
125 pabilities for the detection and quantification of ethylene emissions.

126 Data and code availability

- 127 • Code for retrievals, plume delineation, and quantification is available at https://github.com/jarojuan96/HS_tool. The repository also contains lookup ta-
128 bles of radiance spectra for ethylene, CH_4 , CO_2 , NH_3 , and H_2O . Additional updates
129 related to ethylene retrievals have been implemented for this study relative to Roger
130 et al.¹¹.
- 132 • L1 data from EMIT are open to the public and is available through the Earthdata
133 Search portal:
134 <https://www.earthdata.nasa.gov/data/catalog/lpcloud-emitl1brad-001>

135 Acknowledgements

136 This research is partly funded by the Spanish Ministry of Science, Innovation and Universi-
137 ties (Grant PID2023-148485OB-C21/C22 funded by MCIU/AEI/10.13039/501100011033
138 ERDF, EU).

139 References

- 140 1. Atkinson, R. & Arey, J. Atmospheric degradation of volatile organic compounds.
141 *Chemical Reviews* **103**, 4605–4638 (2003). URL [https://doi.org/10.1021/
142 cr0206420](https://doi.org/10.1021/cr0206420). PMID: 14664626, <https://doi.org/10.1021/cr0206420>.
- 143 2. Amghizar, I., Vandewalle, L. A., Van Geem, K. M. & Marin, G. B. New trends in olefin
144 production. *Engineering* **3**, 171–178 (2017). URL [https://www.sciencedirect.
145 com/science/article/pii/S2095809917302965](https://www.sciencedirect.com/science/article/pii/S2095809917302965).
- 146 3. Franco, B. *et al.* Ethylene industrial emitters seen from space. *Na-
147 ture Communications* **13**, 6452 (2022). URL [https://doi.org/10.1038/
148 s41467-022-34098-8](https://doi.org/10.1038/s41467-022-34098-8).
- 149 4. Clerboux, C. *et al.* The iasi/metop1 mission: First observations and high-
150 lights of its potential contribution to gmes2. *Space Research Today* **168**, 19–
151 24 (2007). URL [https://www.sciencedirect.com/science/article/pii/
152 S0045873207800465](https://www.sciencedirect.com/science/article/pii/S0045873207800465).
- 153 5. Zhang, G. *et al.* Absorption spectroscopy of ethylene near 1.62 μm at high
154 temperatures. *Journal of Quantitative Spectroscopy and Radiative Transfer* **241**,
155 106748 (2020). URL [https://www.sciencedirect.com/science/article/
156 pii/S0022407319306272](https://www.sciencedirect.com/science/article/pii/S0022407319306272).
- 157 6. Sharpe, S. W. *et al.* Gas-phase databases for quantitative infrared spectroscopy.
158 *Applied Spectroscopy* **58**, 1452–1461 (2004).
- 159 7. Connelly, D. S. *et al.* The emit mission information yield for mineral dust radiative
160 forcing. *Remote Sensing of Environment* **258**, 112380 (2021). URL [https://www.
161 sciencedirect.com/science/article/pii/S0034425721000985](https://www.sciencedirect.com/science/article/pii/S0034425721000985).
- 162 8. Thorpe, A. K. *et al.* Attribution of individual methane and carbon diox-
163 ide emission sources using emit observations from space. *Science Advances*
164 **9**, eadh2391 (2023). URL [https://www.science.org/doi/abs/10.1126/
165 sciadv.adh2391](https://www.science.org/doi/abs/10.1126/sciadv.adh2391). [https://www.science.org/doi/pdf/10.1126/sciadv.
166 adh2391](https://www.science.org/doi/pdf/10.1126/sciadv.adh2391).

- 167 9. Roger, J., Guanter, L. & Gorroño, J. Assessing the detection of methane plumes in
168 offshore areas using high-resolution imaging spectrometers. *Atmospheric Measure-*
169 *ment Techniques* **18**, 5545–5567 (2025). URL [https://amt.copernicus.org/
170 articles/18/5545/2025/](https://amt.copernicus.org/articles/18/5545/2025/).
- 171 10. Thompson, D. R. *et al.* Space-based remote imaging spectroscopy of the al-
172 iso canyon ch4 superemitter. *Geophysical Research Letters* **43**, 6571–6578
173 (2016). URL [https://agupubs.onlinelibrary.wiley.com/doi/abs/10.
174 1002/2016GL069079](https://agupubs.onlinelibrary.wiley.com/doi/abs/10.1002/2016GL069079). [https://agupubs.onlinelibrary.wiley.com/doi/
175 pdf/10.1002/2016GL069079](https://agupubs.onlinelibrary.wiley.com/doi/pdf/10.1002/2016GL069079).
- 176 11. Roger, J. *et al.* Remote sensing of ammonia point sources at high spatial resolution
177 with satellite-based imaging spectrometers (2026). URL [https://doi.org/10.
178 31223/X5Q20M](https://doi.org/10.31223/X5Q20M). Preprint.
- 179 12. Bertin, T. *et al.* The hitran2024 methane update. *Journal of Quantitative Spectroscopy*
180 *and Radiative Transfer* **349**, 109736 (2026). URL [https://www.sciencedirect.
181 com/science/article/pii/S002240732500398X](https://www.sciencedirect.com/science/article/pii/S002240732500398X).
- 182 13. Eriksson, P., Buehler, S., Davis, C., Emde, C. & Lemke, O. Arts, the atmospheric
183 radiative transfer simulator, version 2. *Journal of Quantitative Spectroscopy and Ra-*
184 *diative Transfer* **112**, 1551–1558 (2011). URL [https://www.sciencedirect.
185 com/science/article/pii/S0022407311001105](https://www.sciencedirect.com/science/article/pii/S0022407311001105).
- 186 14. Mayer, B. & Kylling, A. Technical note: The libradtran software package for radiative
187 transfer calculations - description and examples of use. *Atmospheric Chemistry and*
188 *Physics* **5**, 1855–1877 (2005). URL [https://acp.copernicus.org/articles/
189 5/1855/2005/](https://acp.copernicus.org/articles/5/1855/2005/).
- 190 15. Dudhia, A. The reference forward model (rfm). *Journal of Quantitative Spec-*
191 *troscopy and Radiative Transfer* **186**, 243–253 (2017). URL [https://www.
192 sciencedirect.com/science/article/pii/S0022407316301029](https://www.sciencedirect.com/science/article/pii/S0022407316301029). Satellite
193 Remote Sensing and Spectroscopy: Joint ACE-Odin Meeting, October 2015.
- 194 16. Foote, M. D. *et al.* Impact of scene-specific enhancement spectra on matched filter
195 greenhouse gas retrievals from imaging spectroscopy. *Remote Sensing of Environ-*
196 *ment* **264**, 112574 (2021). URL [https://www.sciencedirect.com/science/
197 article/pii/S0034425721002947](https://www.sciencedirect.com/science/article/pii/S0034425721002947).
- 198 17. Coheur, P.-F., Clarisse, L., Turquety, S., Hurtmans, D. & Clerbaux, C. Iasi measure-
199 ments of reactive trace species in biomass burning plumes. *Atmospheric Chem-*
200 *istry and Physics* **9**, 5655–5667 (2009). URL [https://acp.copernicus.org/
201 articles/9/5655/2009/](https://acp.copernicus.org/articles/9/5655/2009/).
- 202 18. Kochanov, R. *et al.* Hitran application programming interface (hapi): A comprehensive
203 approach to working with spectroscopic data. *Journal of Quantitative Spectroscopy*

- 204 *and Radiative Transfer* **177**, 15–30 (2016). URL <https://www.sciencedirect.com/science/article/pii/S0022407315302466>. XVIIIth Symposium on High
205 Resolution Molecular Spectroscopy (HighRus-2015), Tomsk, Russia.
206
- 207 19. Frankenberg, C. *et al.* Airborne methane remote measurements reveal heavy-
208 tail flux distribution in four corners region. *Proceedings of the National Academy*
209 *of Sciences* **113**, 9734–9739 (2016). URL [https://www.pnas.org/doi/abs/](https://www.pnas.org/doi/abs/10.1073/pnas.1605617113)
210 [10.1073/pnas.1605617113](https://www.pnas.org/doi/pdf/10.1073/pnas.1605617113). [https://www.pnas.org/doi/pdf/10.1073/](https://www.pnas.org/doi/pdf/10.1073/pnas.1605617113)
211 [pnas.1605617113](https://www.pnas.org/doi/pdf/10.1073/pnas.1605617113).
- 212 20. Varon, D. J. *et al.* Quantifying methane point sources from fine-scale satellite obser-
213 vations of atmospheric methane plumes. *Atmospheric Measurement Techniques* **11**,
214 5673–5686 (2018). URL [https://amt.copernicus.org/articles/11/5673/](https://amt.copernicus.org/articles/11/5673/2018/)
215 [2018/](https://amt.copernicus.org/articles/11/5673/2018/).
- 216 21. Guanter, L. *et al.* Multisatellite data depicts a record-breaking methane leak
217 from a well blowout. *Environmental Science & Technology Letters* **11**, 825–830
218 (2024). URL <https://doi.org/10.1021/acs.estlett.4c00399>. <https://doi.org/10.1021/acs.estlett.4c00399>.
219 <https://doi.org/10.1021/acs.estlett.4c00399>.
- 220 22. Gorroño, J., Pei, Z., Valverde, A. & Guanter, L. Considering the observation and illumi-
221 nation angular configuration for an improved detection and quantification of methane
222 emissions. *Atmospheric Measurement Techniques* **19**, 1245–1257 (2026). URL
223 <https://amt.copernicus.org/articles/19/1245/2026/>.
- 224 23. Gorroño, J., Pei, Z. & Guanter, L. Benchmark simulations for methane emissions vali-
225 dation and sensitivity studies (2026). URL [https://doi.org/10.5281/zenodo.](https://doi.org/10.5281/zenodo.18161182)
226 [18161182](https://doi.org/10.5281/zenodo.18161182).
- 227 24. Molod, A. *et al.* The geos-5 atmospheric general circulation model: Mean climate
228 and development from merra to fortuna. [https://portal.nccs.nasa.gov/](https://portal.nccs.nasa.gov/datashare/gmao/geos-fp/das/)
229 [datashare/gmao/geos-fp/das/](https://portal.nccs.nasa.gov/datashare/gmao/geos-fp/das/) (2012). Accessed: 12 June 2026.
- 230 25. Roger, J. *et al.* High-resolution methane mapping with the enmap satellite imaging
231 spectroscopy mission. *IEEE Transactions on Geoscience and Remote Sensing* **62**,
232 1–12 (2024).
- 233 26. Green, R. O. *et al.* Imaging spectroscopy and the airborne visible/infrared
234 imaging spectrometer (aviris). *Remote Sensing of Environment* **65**, 227–248
235 (1998). URL [https://www.sciencedirect.com/science/article/pii/](https://www.sciencedirect.com/science/article/pii/S0034425798000649)
236 [S0034425798000649](https://www.sciencedirect.com/science/article/pii/S0034425798000649).
- 237 27. Guanter, L. *et al.* The enmap spaceborne imaging spectroscopy mission for earth
238 observation. *Remote Sensing* **7**, 8830–8857 (2015). URL [https://www.mdpi.](https://www.mdpi.com/2072-4292/7/7/8830)
239 [com/2072-4292/7/7/8830](https://www.mdpi.com/2072-4292/7/7/8830).

- 240 28. Loizzo, R. *et al.* Prisma: The italian hyperspectral mission. In *IGARSS 2018 - 2018*
241 *IEEE International Geoscience and Remote Sensing Symposium*, 175–178 (2018).
- 242 29. Liu, Y.-N. *et al.* The advanced hyperspectral imager: Aboard china’s gaofen-5 satel-
243 lite. *IEEE Geoscience and Remote Sensing Magazine* **7**, 23–32 (2019).
- 244 30. Duren, R. *et al.* The carbon mapper emissions monitoring system. *Atmospheric Mea-*
245 *surement Techniques* **18**, 6933–6958 (2025). URL [https://amt.copernicus.](https://amt.copernicus.org/articles/18/6933/2025/)
246 [org/articles/18/6933/2025/](https://amt.copernicus.org/articles/18/6933/2025/).
- 247 31. Celesti, M. *et al.* The copernicus hyperspectral imaging mission for the environment
248 (chime): Status and planning. In *IGARSS 2022 - 2022 IEEE International Geoscience*
249 *and Remote Sensing Symposium*, 5011–5014 (2022).

250 **Competing interests:** The authors declare no competing interests.

251 **List of Figures**

252 1 Cross section spectra of methane (blue) and ethylene (red) at P = 1 atm
253 and T = 298.1 K. 10

254 2 Examples of two ethylene plumes overlaid on high-resolution Google Earth
255 images (© Google Earth; data provider: Airbus). From left to right, we find
256 a plume in Saudi Arabia and another one in Iraq. Both plumes were char-
257 acterized using EMIT data and were originated from industrial sources. De-
258 tails of the ethylene concentration-path length enhancement levels, acqui-
259 sition date, source coordinates, and emission quantification can be found
260 for each plume. 11

261 3 Analysis of potential ethylene emission correlation with other gas retrievals
262 for the Saudi Arabia (top) and Iraq (bottom) plumes. Starting from the
263 top: radiance reference band, ethylene, and CH₄ retrievals. The ethylene
264 source is marked with a red dot in all the panels. Note that the plume
265 orientation differs from that shown in Figure 2, where the retrievals are
266 georeferenced. 12

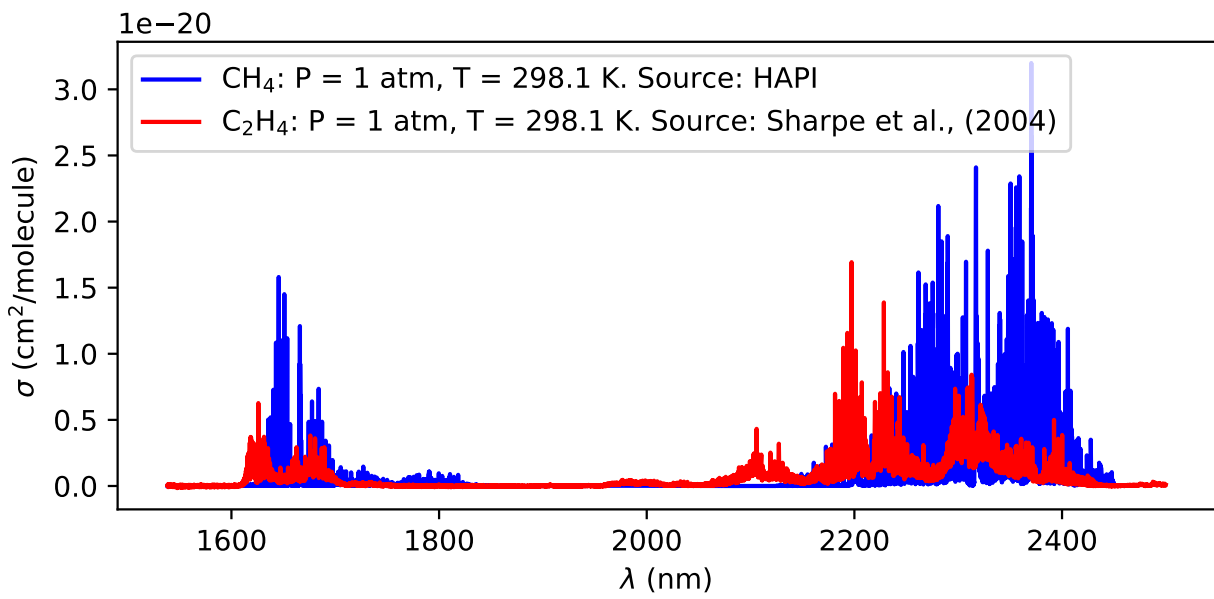


Figure 1: Cross section spectra of methane (blue) and ethylene (red) at P = 1 atm and T = 298.1 K.

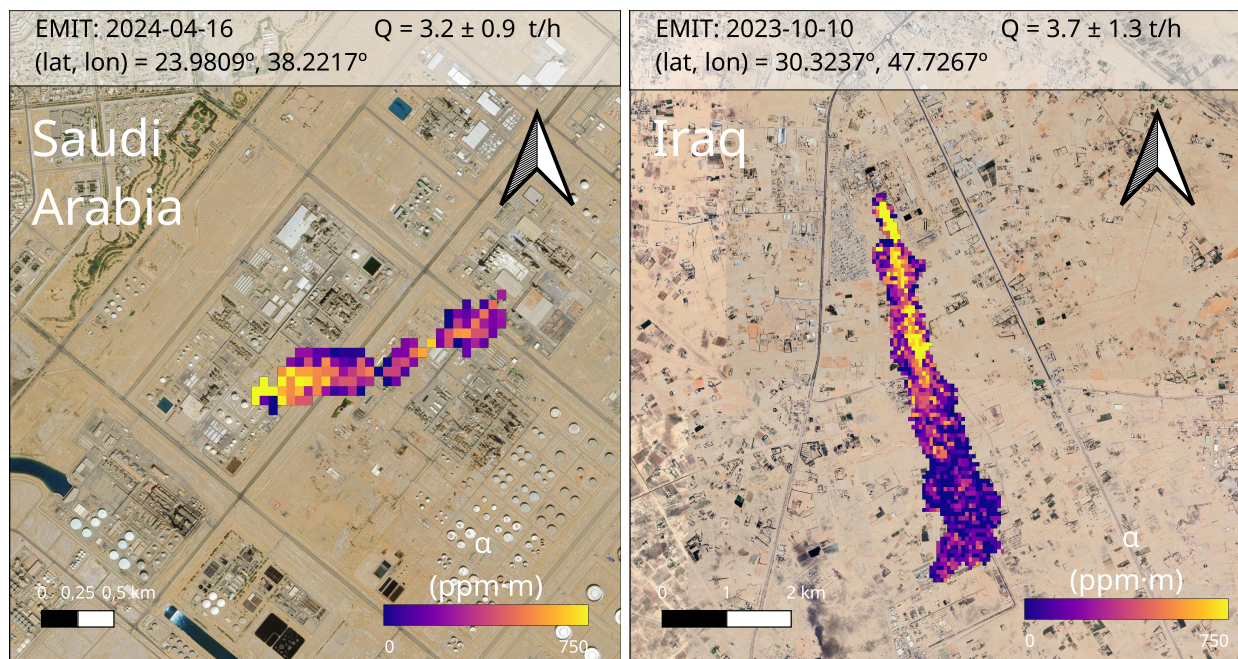


Figure 2: Examples of two ethylene plumes overlaid on high-resolution Google Earth images (© Google Earth; data provider: Airbus). From left to right, we find a plume in Saudi Arabia and another one in Iraq. Both plumes were characterized using EMIT data and were originated from industrial sources. Details of the ethylene concentration-path length enhancement levels, acquisition date, source coordinates, and emission quantification can be found for each plume.

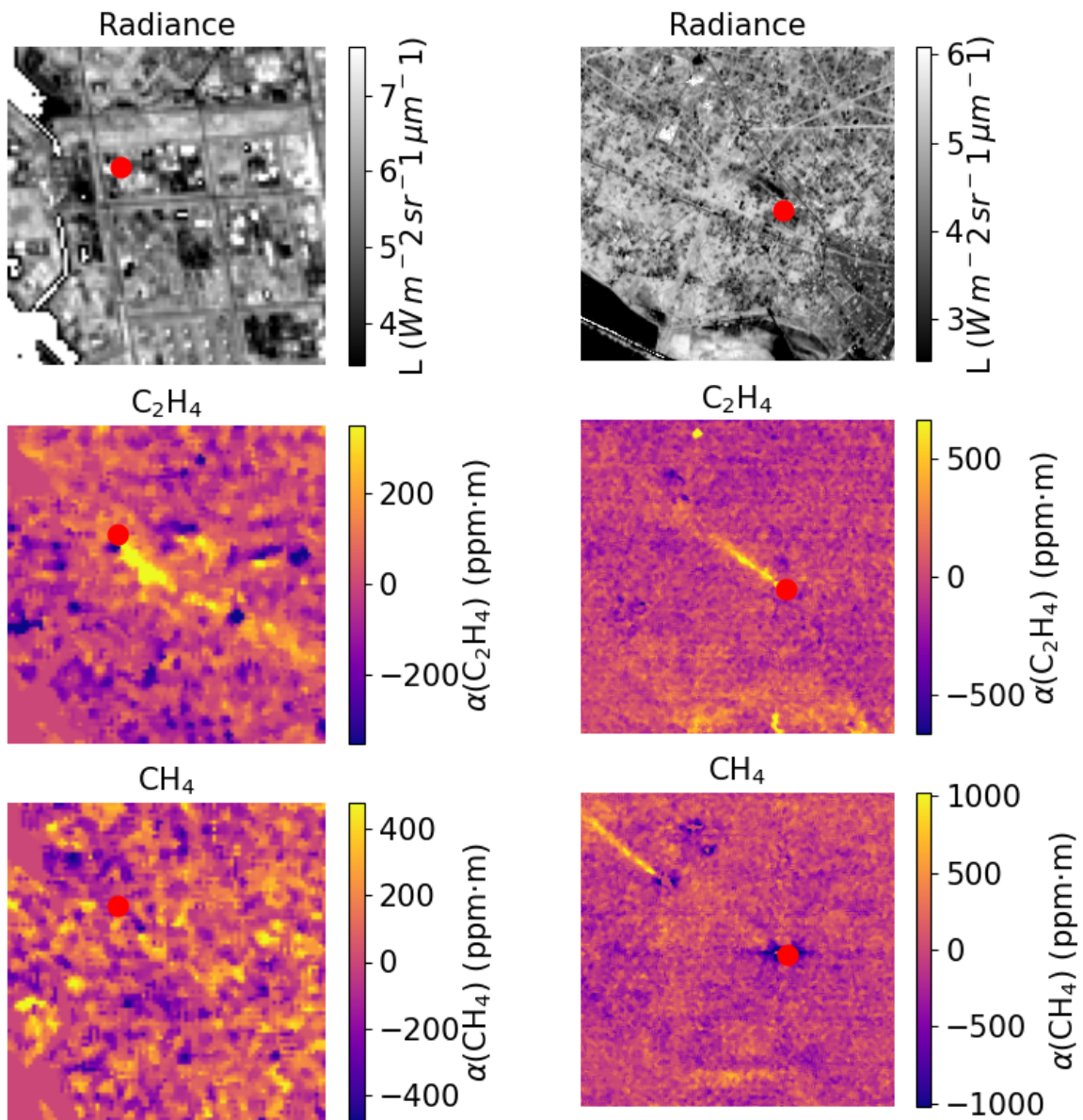


Figure 3: Analysis of potential ethylene emission correlation with other gas retrievals for the Saudi Arabia (top) and Iraq (bottom) plumes. Starting from the top: radiance reference band, ethylene, and CH_4 retrievals. The ethylene source is marked with a red dot in all the panels. Note that the plume orientation differs from that shown in Figure 2, where the retrievals are georeferenced.